# Precision Measurement of the Spin Structure Function $g_2$ of the Proton at $Q^2 = 0.8$ and $2.0$ GeV$^2$


X. Zheng
*Argonne National Lab, Argonne, IL 60439*

J.-P. Chen, R. Ent, J. Gomez, D. W. Higinbotham, M. Jones, W. Melnitchouk, R. Michaels, G. Warren
*Jefferson Lab, Newport News, VA 23606*

A. T. Katramatou, G. G. Petratos
*Kent State University, Kent, OH 44242*

W. Korsch
*University of Kentucky, Lexington, KY 40506*

L. Gamberg
*Penn State University, Berks, Reading, PA 19610*

R. Gilman, X. Jiang
*Rutgers University, Piscataway, NJ 08855*

F. Butaru, Seonho Choi (Cospokesperson), A. Lukhanin, Z.-E. Meziani (Cospokesperson), K. Slifer, P. Solvignon, H. Yao
*Temple University, Philadelphia, PA 19122*

D. G. Crabb (Cospokesperson), D. Day, N. Liyanage, O. Rondon-Aramayo
*University of Virginia, Charlottesville, VA 22901*

D. Armstrong, T. Averett
*College of William and Mary, Williamsburg, VA 23185*

Contact: Seonho Choi (choi@jlab.org)

April 28, 2003

**Abstract**

We propose to make a precision measurement of spin dependent asymmetries for the inclusive reaction on the proton $\vec{p}(\vec{e}, e')$ from the pion production threshold up to an invariant mass $W = 2.4$ GeV at two different values of $Q^2$, 0.8 and 2.0 GeV$^2$. We shall use polarized proton target both in transverse and longitudinal configurations. The results on the spin structure functions $g_1(x, Q^2)$ and $g_2(x, Q^2)$ will enable us to test the Burkhardt-Cottingham sum rule on the proton and evaluate the $d_2(Q^2)$. This quantity is a measure of higher twist effect in $g_2(x, Q^2)$ structure function. The previous measurement at SLAC showed a possible violation of the BC sum rule at $Q^2 = 5$ GeV$^2$ and positive, non-zero value for $d_2(Q^2)$.

# 1 Introduction and Motivation

With the advent of polarized electron beam and targets, the study of spin structure of the nucleon enriched our understanding of Quantum ChromoDynamics (QCD), the underlying theory of the strong interaction. The spin structure of the nucleon is described in terms of two structure functions, $g_1(x, Q^2)$ and $g_2(x, Q^2)$. In the parton model, $g_1(x, Q^2)$ has a simple interpretation as unpolarized structure functions ($F_1$ and $F_2$) do, but $g_2(x, Q^2)$ doesn't.

On the other hand, at high $Q^2$, where contribution of twist higher than 3 are negligible, Operator Product Expansion (OPE) [1, 2] shows that $g_1(x, Q^2)$ contains twist-2 contribution only, whereas $g_2(x, Q^2)$ contains both twist-2 and twist-3 contributions, of which the simplest case is one gluon exchange during the scattering process. The twist-3 contributions are a direct manifestation of quark-gluon interaction and quark masses. Its measurement and comparison with theory is another important test of QCD.

The higher-twist effect of $g_2(x, Q^2)$ can be quantified by $d_2(Q^2)$,

$$d_2(Q^2) = \int_0^1 x^2 \left[2g_1(x, Q^2) + 3g_2(x, Q^2)\right] dx \quad (1)$$

$$= 3\int_0^1 x^2 \overline{g_2}(x, Q^2)\, dx, \quad (2)$$

where

$$\overline{g_2}(x, Q^2) = g_2(x, Q^2) - g_2^{WW}(x, Q^2) \quad (3)$$

$$g_2^{WW}(x, Q^2) = -g_1(x, Q^2) + \int_x^1 \frac{g_1(y, Q^2)}{y}\, dy. \quad (4)$$

Here $g_2^{WW}(x, Q^2)$, derived by Wandzura-Wilczek [3], is the twist-2 contribution to $g_2(x, Q^2)$.

At high $Q^2$, $d_2(Q^2)$ is a reduced matrix element that is related to the induced color electric and magnetic polarizabilities $\chi_E$ and $\chi_B$ when a nucleon is polarized [4, 5],

$$d_2 = \frac{1}{8}(\chi_E + 2\chi_B). \quad (5)$$

The sign of $\chi_B$ reflects the direction of the color magnetic field with respect to the polarization of the nucleon.

At very low $Q^2$, recent work has shown that $d_2(Q^2)$ can be expressed as a linear combination of transverse ($\gamma_0$) and longitudinal ($\delta_{LT}$) nucleon spin polariz-

abilities [6],

$$d_2(Q^2) = \frac{Q^6}{16M^2\alpha_{\rm em}}\left[3\delta_{LT}(Q^2) - \gamma_0(Q^2)\right], \tag{6}$$

where $\delta_{LT}$ and $\gamma_0$ are generalized forward spin polarizabilities, longitudinal-transverse and purely transverse, respectively.

Understanding the transition from "*color*" electric and magnetic polarizabilities to "*spin*" polarizabilities in the framework of QCD and comparing with the experimental results would be another key check for our understanding of QCD.

The fact that the leading order to $g_2(x, Q^2)$ contains twist-3 contributions has another implication for the sum rule. While the Bjorken sum rule [7, 8] can be re-derived using the OPE, similar sum rule for $g_2(x, Q^2)$ *cannot*.

The sum rule for $g_2(x, Q^2)$, reads

$$\int_0^1 g_2(x, Q^2)\, dx = 0. \tag{7}$$

and first derived by Burkhardt and Cottingham (BC) [9] in 1969, based on the dispersion relation and the asymptotic behavior of the corresponding Compton amplitude. As mentioned earlier, the BC sum rule can not be confirmed with the OPE [10]. On the other hand, vanishing higher-twist effect *do* imply the BC sum rule.

Using $g_2(x, Q^2)$ and also separating elastic contribution, the BC sum rule reads

$$\begin{aligned}
\Gamma_2(Q^2) &= \int_0^1 g_2(x, Q^2)\, dx & (8)\\
&= \int_0^{x_0} g_2(x, Q^2)\, dx - \frac{\tau}{2(1+\tau)} G_M(Q^2)\left[G_M(Q^2) - G_E(Q^2)\right] & (9)\\
&= 0 & (10)
\end{aligned}$$

where $x_0$ is the value of $x$ corresponding to pion production threshold, $\tau = Q^2/4M^2$, and $G_E(Q^2), G_M(Q^2)$ are electric and magnetic form factors of the nucleon.

For the sake of convenience, let us define

$$\Gamma_2^{\rm inel}(Q^2) = \int_0^{x_0} g_2(x, Q^2)\, dx \tag{11}$$

which contains only the inelastic contribution to $g_2(x, Q^2)$. Burkhardt and Cottingham claimed that this sum rule is valid for all values of $Q^2$. Often, $Q^2 \to \infty$

limit, where $G_E$ and $G_M$ are negligible, is taken. The BC sum rule is then presented as

$$\Gamma_2^{\rm inel}(Q^2) = 0 \quad \text{as} \quad Q^2 \to \infty. \tag{12}$$

Since the BC sum rule has been postulated, there have been a number of issues concerning the validity of the sum rule. While Operator Product Expansion (OPE) at high $Q^2$ provides a solid background for the sum rules involving $g_1(x)$, OPE can not be used for the BC sum rule and a number of authors raised questions on the very starting assumptions in the derivation by Burkhardt and Cottingham [10, 11, 12, 2]. In one scenario, if $g_2(x)$ is divergent faster than $1/x$ as $x \to 0$, the integral of $g_2(x)$ is divergent and there is no sum rule.

However, a number of simple models *do* satisfy the BC sum rule and it has been shown by an explicit calculation, that it is fulfilled in higher order QCD [13, 14]. Furthermore, within the light-cone OPE, there is no twist-3 operator for the first moment of $g_2(x, Q^2)$ [15] satisfying the BC sum rule. This is a hint, though no proof that the BC sum rule holds.

In the other scenario [2], $g_2(x)$ can have a $\delta$ function at $x = 0$. In this case, the BC sum rule holds formally, but it would be impossible to verify it experimentally since a $\delta$ function at $x = 0$ is not detectable. So the measured $g_2(x)$ would appear to violate the BC sum rule.

When an experiment finds a violation of the BC sum rule, it is not easy to distinguish the two previous possibilities. However, the recent result on the neutron from JLab shows that the BC sum rule seems to be satisfied already in low $Q^2$ region at least for the neutron. If the BC sum rule *does* hold, this result suggests that any *exotic* behavior of $g_2(x)$ near $x = 0$ gives very small, if not zero, contribution to the BC sum rule.

With the advent of polarized electron beam and targets, there have been a series of experiments to measure the spin structure functions of the proton and the neutron from DESY, CERN, SLAC and Jefferson Lab. However, most of the earlier experiments focused on the $g_1(x, Q^2)$ structure function in the Deep Inelastic Scattering (DIS) region. As a result, the data for $g_2(x, Q^2)$ are scarce. SLAC E155X [16] has produced a wealth of data mainly at high $Q^2$ for $g_1(x, Q^2)$ and $g_2(x, Q^2)$ on both the proton and the neutron. Recently, Jefferson Lab has provided low to intermediate $Q^2$ data on the neutron and the proton [17, 18, 19, 20, 21, 22, 23].

The first experimental test of the BC sum rule is from SLAC E155X experiment [16]. For the proton, their result reads

$$\Gamma_2^{\rm inel}(\text{proton}, Q^2 = 5\ \text{GeV}^2) = 0.024 \pm 0.008 \pm 0.003. \tag{13}$$

At this $Q^2$, the elastic contribution is negligible and $\Gamma_2^{\rm inel}$ can be compared directly with zero for the BC sum rule. The authors concluded that their result on the proton is inconsistent with the BC sum rule.

A measurement of the neutron structure functions at $Q^2$ below 1 GeV$^2$, JLab E94010, has also produced interesting results regarding to the BC sum rule on the neutron. Figure 1 shows the summary of currently available experimental data for the BC sum rule. While the results for the neutron from SLAC and JLab are consistent with zero within errors, the only proton result shows a clear deviation from zero. It is worth mentioning that JLab results are integrated up to $W = 2$ GeV and do not include DIS contribution, which has been estimated using $g_2^{WW}(x, Q^2)$ and plotted as negative error band (dark gray, or magenta region) in the Figure. Within the errors, the results on the neutron seem to satisfy the BC sum rule.

For the proton, there is no high precision data for $g_2(x, Q^2)$ other than the SLAC E155X measurement, especially in the intermediate $Q^2$ region. The data analysis of JLab E91023 and E01006 [17, 22] are still in progress and the results should be available soon.

While waiting for the results, the MAID model has been used to evaluate $\Gamma_2(Q^2)$ for $Q^2 < 5$ GeV$^2$. First of all, the MAID model has been checked against available neutron data [24] (dot-dashed curve in Figure 1) and a good agreement has been found. However, for the proton, the same model predicts significant violation of the BC sum rule in the same $Q^2$ region. The dashed curve in the Figure shows MAID prediction while dotted line below zero axis shows the elastic contribution. The sum of these two (solid line) should be compared to zero for the BC sum rule. Although MAID is just a model, it would be very interesting to check the BC sum rule for the proton for the $Q^2$ range where MAID predicts a large violation, especially when the same model predicts a verified sum rule for the neutron which is in agreement with the measurement.

If the measurement gives a result close to zero as in the case of the neutron, we are one step closer to the BC sum rule and the validity of the SLAC E155X measurement can perhaps be questioned. On the other hand, if the result on the proton shows significant deviation from zero giving the correct trend to the SLAC E155X point, one of the major questions would be why there is a significant difference between the neutron and the proton.

Similar to the situation for the BC sum rule, there is one available measurement of $d_2(Q^2)$ for the proton and the neutron at $Q^2 = 5$ GeV$^2$ from SLAC E155X and data for the neutron from JLab E94010 be;pw $Q^2 = 1$ GeV$^2$. Again, results from JLab E91023 and E01006 [17, 22] on the proton will be available soon.

Figure 2 summarizes current status of experimental measurement of $d_2(Q^2)$.

The data from JLab E94010 show a trend which suggests approaching zero at high $Q^2$ in agreement with the MAID model. It is interesting that the MAID model predicts reasonably well both the trend and the magnitude of the neutron data at low $Q^2$ region. For the case of $d_2(Q^2)$, MAID model shows less dramatic difference between the proton and the neutron than it does for the BC sum rule. However, between $Q^2 = 1$ and 5 GeV$^2$, while MAID model predicts smooth decrease to zero for the neutron, it shows change of sign and coming back to zero for the proton. Especially, MAID model predicts a sign change between $Q^2 = 1$ and 2 GeV$^2$, making the current proposal all the more interesting. Results from JLab E01006 [22] will give results at $Q^2 \simeq 1.3$ GeV$^2$ and two more measurements below and above this $Q^2$ will give a clear picture of $d_2(Q^2)$ in this possibly interesting region. More theoretical work is needed to understand the transition between the high $Q^2$ region where $d_2(Q^2)$ is interpreted in terms of color polarizabilities and the low $Q^2$ region where it is rather related to spin polarizabilities.

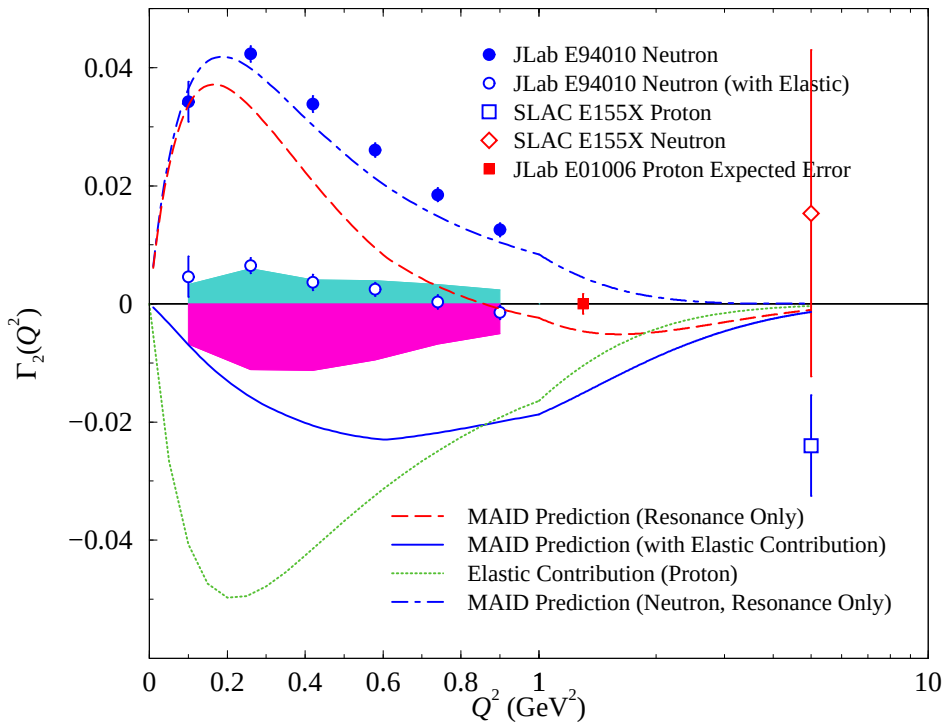


Figure 1: Experimental data for the Burkhardt-Cottingham sum rule. For better presentation of available data, $Q^2$ axis is linear from 0 to 1 GeV$^2$ and logarithmic from 1 to 10 GeV$^2$. Filled circles are for the neutron from JLab E94010 with light gray (above the zero axis) band as experimental systematic error. Another systematic error band (dark gray, below the zero axis) shows an estimate of DIS contribution not measured by JLab E94010. When elastic contributions are added, open circles are obtained indicating possible satisfaction of the BC sum rule within errors. Open diamond and open square are for the neutron and the proton respectively from SLAC E155X. Filled square points at $Q^2$=1.3 GeV$^2$ shows expected error from JLab E01006. Dot-dashed line shows MAID prediction for the neutron in very good agreement with the measurement. Dashed line is for the proton and after adding elastic contribution (dotted line below zero axis), the solid line is obtained and should be compared with zero for the BC sum rule.

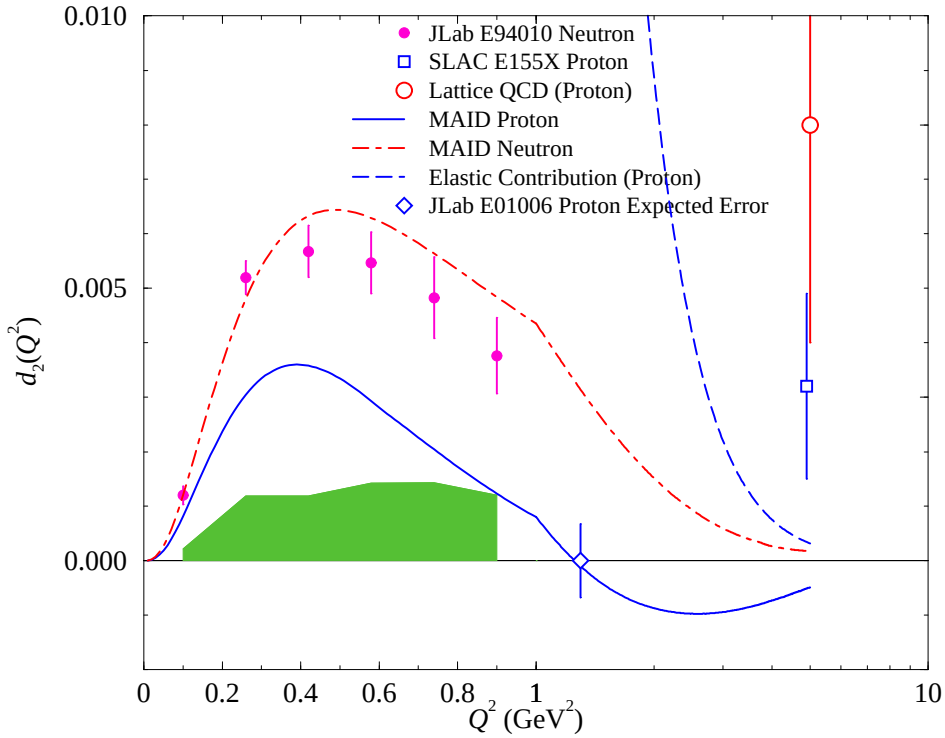


Figure 2: Experimental data for $d_2(Q^2)$ from $Q^2 = 0$ to 5 GeV$^2$. For better presentation of available data, $Q^2$ axis is linear from 0 to 1 GeV$^2$ and logarithmic from 1 to 10 GeV$^2$. Filled circles are for the neutron from JLab E94010 with gray band as systematic error. Open square is the result from SLAC E155X. Open diamond at $Q^2 = 1.3$ GeV$^2$ shows expected error from JLab E01006. Dot-dashed and solid lines are MAID prediction for the neutron and the proton respectively. The lattice QCD calculation for the proton is shown in open circle. When comparing the experimental data with lattice QCD calculation, it is important to include elastic contribution, shown in dashed line for the proton. For example, for $Q^2 = 2.0$ GeV$^2$, it is quite surprising that the sum of the MAID prediction and the elastic contribution is almost equal to the Lattice QCD prediction.

# 2 Separation of $g_1(x)$ and $g_2(x)$

When the target spin lies in the scattering plane defined by the incoming and outgoing electrons, the difference of the cross sections for the two beam helicities is given by,

$$\frac{d^2\sigma^{\downarrow,S}}{dE'd\Omega} - \frac{d^2\sigma^{\uparrow,S}}{dE'd\Omega} = \Delta\sigma_{\parallel}\cos\alpha + \Delta\sigma_{\perp}\sin\alpha, \tag{14}$$

where $\alpha$ is the angle of the target spin with respect to the incoming electron direction and $\Delta\sigma_{\parallel}$ and $\Delta\sigma_{\perp}$ are

$$\Delta\sigma_{\parallel} = \frac{d^2\sigma}{dE'd\Omega}(\downarrow\Uparrow - \uparrow\Uparrow) \tag{15}$$

$$= \frac{4\alpha^2}{MQ^2}\frac{E'}{\nu E}\left[(E + E'\cos\theta)g_1 - \frac{Q^2}{\nu}g_2\right] \tag{16}$$

$$\Delta\sigma_{\perp} = \frac{d^2\sigma}{dE'd\Omega}(\downarrow\Rightarrow - \uparrow\Rightarrow) \tag{17}$$

$$= \frac{4\alpha^2\sin\theta}{MQ^2}\frac{E'^2}{E}\frac{1}{\nu^2}(\nu g_1 + 2Eg_2). \tag{18}$$

In short, $\Delta\sigma_{\parallel}$ and $\Delta\sigma_{\perp}$ are cross section differences when the target spin is longitudinal ($\alpha = 0$) or transverse ($\alpha = 90^\circ$) to the incoming electron direction.

It is ideal to have longitudinal and transverse configuration. However, as discussed later, the configuration of the target magnet and big scattering angle makes $\alpha = 80^\circ$ to be the best compromise. In this case, the measurements in this *quasi*-transverse mode will be contaminated by $\cos 80^\circ \simeq 17\%$ of the longitudinal mode. This will make our measurements slightly less sensitive to $g_2$ than in the ideal case, but can be overcome with increased time in *quasi*-transverse configuration. From now on, "transverse" in this proposal means this *quasi*-transverse configuration.

We intend to measure spin dependent asymmetries for four different configurations of the beam and target polarization directions:

$$(\downarrow\Uparrow), \quad (\uparrow\Downarrow), \quad (\downarrow\Rightarrow), \quad (\uparrow\Rightarrow),$$

where the first arrow indicates the direction of the beam polarization while the second (double) arrow shows the orientation of the target polarization (either longitudinal or transverse to the beam line).

The asymmetries for both configurations are defined as

$$A_{\parallel} = \frac{\sigma_{\downarrow\Uparrow} - \sigma_{\uparrow\Uparrow}}{\sigma_{\downarrow\Uparrow} + \sigma_{\uparrow\Uparrow}} \quad A'_{\perp} = \frac{\sigma_{\downarrow\Rightarrow} - \sigma_{\uparrow\Rightarrow}}{\sigma_{\downarrow\Rightarrow} + \sigma_{\uparrow\Rightarrow}}, \tag{19}$$

where $\sigma$'s are shorthand notation for differential cross sections $\frac{d^2\sigma}{dE'd\Omega}$. Using $A'_{\perp} = A_{\perp}\sin\alpha + A_{\parallel}\cos\alpha$, with $\alpha = 80^{\circ}$, $A_{\perp}$ can be obtained as

$$A_{\perp} = \frac{A'_{\perp} - A_{\parallel}\cos\alpha}{\sin\alpha}. \tag{20}$$

Now using the unpolarized cross section ($\sigma_0$) measured in another experiment [25], the difference of the differential cross sections can be obtained as

$$\frac{d^2\sigma}{dE'd\Omega}(\downarrow\Uparrow - \uparrow\Uparrow) = 2A_{\parallel}\sigma_0 \tag{21}$$

$$\frac{d^2\sigma}{dE'd\Omega}(\downarrow\Rightarrow - \uparrow\Rightarrow) = 2A_{\perp}\sigma_0 \tag{22}$$

$$\tag{23}$$

It is straightforward to extract $g_1(x)$ and $g_2(x)$ from these two independent linear combinations.

# 3 Kinematics

To check the BC sum rule, it is very important to perform an integral of $g_2(x)$ at *constant* $Q^2$. One of the possibilities why SLAC E155X measurement shows apparent violation of the BC sum rule is that their $Q^2$ is not constant. As shown in Figure 5, their $Q^2$ varies from about 0.8 GeV$^2$ to 8 GeV$^2$.

Two values of $Q^2$ has been picked up: 2 GeV$^2$ and 0.8 GeV$^2$. These two values of $Q^2$ provide the two extremes within reasonable experimental conditions. Data at both values of $Q^2$ can show the trend as we move to larger $Q^2$ values. And $Q^2 = 0.8$ GeV$^2$ point is interesting in itself since MAID model predicts pretty large violation of the BC sum rule.

Additional kinematics have been chosen in order to extend the kinematic region of the JLab E01006. The previous experiment has a coverage at $Q^2 \simeq 1.3$ GeV$^2$ with a missing mass $W$ up to $\sim 1.9$ GeV. With a slight increase of the beam time, it is possible to extend the coverage up to $W = 2.4$ GeV. This *extension* has been achieved with a 5.7 GeV beam energy at smaller spectrometer angles.

One minor complication comes from the target geometry in transverse configuration. In this configuration, the polarized proton target has only $\pm 17^\circ$ of opening angle and does not allow large angle ($\sim 22^\circ$) required for the high $Q^2$ measurement. To accommodate such a large scattering angle, the target will be rotated to $80^\circ$ with respect to the beam line, instead of $90^\circ$ in the case of true transverse configuration. This minor change in angle increases the statistical error on the extracted $g_2$ very slightly.

For the transverse configuration, the strong magnetic field (4.8T, or $\int Bdl = 1.4$ Tm) is almost perpendicular to the direction of the electrons and bends outgoing electrons toward the beam line. When calculating the actual kinematics at the reaction vertex, this effect has been taken into account. The effect is small at 5.7 and 4.00 GeV kinematics, on the order of a few degrees, but becomes quite large (up to $\simeq 8^\circ$) at 3.00 GeV kinematics where the momenta of the outgoing electrons are low. For longitudinal configuration, although scattered electrons have a small momentum component perpendicular to the longitudinal magnetic field, this bending effect is negligible.

To minimize the required time, we intend to change spectrometer angles ($\theta$) and the energy ($E'$) of the scattered electrons keeping $Q^2$ constant. And one more measurement at lower energy (not at constant $Q^2$ and with compromised statistics) has been added for the purpose of radiative corrections only. Tables 1 and 2 summarizes the required kinematics. And Figures 3 and 4 shows the actual coverage in $Q^2$ and $W$ with these kinematics. Each diamond shaped region shows the actual coverage by one spectrometer setting.

As Figure 6 shows, the previous experiment, JLab E01006 has covered the resonance region from $W \simeq 0.9$ to 1.9 GeV with varying $Q^2$ centered around 1.3 GeV$^2$. This kinematics corresponds to $d_2(Q^2)$ zero crossing point according to MAID model (Figure 2). Our lower $Q^2$ kinematics at 0.8 GeV$^2$ is necessary to increase our lever arm in order to verify the actual zero crossing, if indeed it *does* happen.

The lowest $x$ value achievable with this proposal is limited due to a combination of the beam energy and maximum scattering angle and does not go as low as SLAC E155X. However, SLAC result at the same $Q^2$ (0.8, 1.3 and 2.0 GeV$^2$, see Figure 5) can be used to complement our lack of data at small $x$ region.

| $E_{\rm beam}$ (GeV) | $E'$ (GeV) | Spectrometer Angle ($^\circ$) | $W$ (GeV) | $x_{\rm Bj}$ |
|---|---|---|---|---|
| 5.70 ($Q^2 = 2$ GeV$^2$) | 4.2000 | 15.8492 | 1.3020 | 0.7105 |
| | 3.5778 | 17.1551 | 1.6920 | 0.5022 |
| | 3.0477 | 18.5568 | 1.9640 | 0.4018 |
| | 2.5962 | 20.0596 | 2.1690 | 0.3434 |
| | 2.2116 | 21.6655 | 2.3295 | 0.3055 |
| 5.70 ($Q^2 = 1.3$ GeV$^2$) | 3.5000 | 13.5704 | 1.9258 | 0.3149 |
| | 2.9815 | 14.6539 | 2.1638 | 0.2548 |
| | 2.5398 | 15.8039 | 2.3475 | 0.2192 |
| 4.00 ($Q^2 = 0.8$ GeV$^2$) | 3.2300 | 12.5998 | 1.2350 | 0.5537 |
| | 2.7515 | 13.6122 | 1.5567 | 0.3415 |
| | 2.3439 | 14.6773 | 1.7855 | 0.2574 |
| | 1.9966 | 15.7912 | 1.9595 | 0.2128 |
| | 1.7008 | 16.9468 | 2.0964 | 0.1854 |
| | 1.4488 | 18.1331 | 2.2063 | 0.1671 |
| | 1.2342 | 19.3349 | 2.2958 | 0.1541 |
| | 1.0514 | 20.5267 | 2.3693 | 0.1446 |
| 3.00 | 2.5000 | 12.5 | 1.1340 | 0.5677 |
| | 2.1296 | | 1.4249 | 0.2960 |
| | 1.8141 | | 1.6314 | 0.1997 |
| | 1.5454 | | 1.7876 | 0.1518 |
| | 1.3164 | | 1.9096 | 0.1244 |
| | 1.1214 | | 2.0066 | 0.1076 |
| | 0.9553 | | 2.0844 | 0.0972 |
| | 0.8137 | | 2.1469 | 0.0911 |
| | 0.6932 | | 2.1981 | 0.0872 |
| | 0.5905 | | 2.2540 | 0.0711 |
| | 0.5030 | | 2.3005 | 0.0584 |

Table 1: Required kinematics for the transverse configuration with relevant variables. The data with beam energy 3 GeV are taken for the purpose of radiative corrections only and no attempt was made to keep $Q^2$ constant.

| $E_{\rm beam}$ (GeV) | $E'$ (GeV) | Spectrometer Angle ($^\circ$) | $W$ (GeV) | $x_{\rm Bj}$ |
|---|---|---|---|---|
| 5.70 ($Q^2 = 2$ GeV$^2$) | 4.2000 | 16.6188 | 1.3020 | 0.7105 |
| | 3.5778 | 18.0169 | 1.6920 | 0.5022 |
| | 3.0477 | 19.5352 | 1.9640 | 0.4018 |
| | 2.5962 | 21.1842 | 2.1691 | 0.3434 |
| | 2.2116 | 22.9755 | 2.3295 | 0.3055 |
| 5.70 ($Q^2 = 1.4$ GeV$^2$) | 3.5000 | 14.6661 | 1.9258 | 0.3149 |
| | 2.9815 | 15.8976 | 2.1637 | 0.2548 |
| | 2.5398 | 17.2346 | 2.3475 | 0.2192 |
| 4.00 ($Q^2 = 0.8$ GeV$^2$) | 3.2300 | 14.2945 | 1.2350 | 0.5537 |
| | 2.7515 | 15.4949 | 1.5567 | 0.3415 |
| | 2.3439 | 16.7966 | 1.7855 | 0.2574 |
| | 1.9966 | 18.2100 | 1.9596 | 0.2128 |
| | 1.7008 | 19.7448 | 2.0964 | 0.1854 |
| | 1.4488 | 21.4121 | 2.2063 | 0.1671 |
| | 1.2342 | 23.2236 | 2.2958 | 0.1541 |
| | 1.0514 | 25.1920 | 2.3693 | 0.1446 |
| 3.00 | 2.5000 | 15.32 | 1.1338 | 0.5681 |
| | 2.1296 | | 1.4351 | 0.2780 |
| | 1.8141 | | 1.6489 | 0.1738 |
| | 1.5454 | | 1.8112 | 0.1207 |
| | 1.3164 | | 1.9388 | 0.0888 |
| | 1.1214 | | 2.0412 | 0.0678 |
| | 0.9553 | | 2.1246 | 0.0531 |
| | 0.8137 | | 2.1930 | 0.0423 |
| | 0.6932 | | 2.2498 | 0.0341 |
| | 0.5905 | | 2.2970 | 0.0278 |
| | 0.5030 | | 2.3360 | 0.0233 |

Table 2: Required kinematics for the longitudinal configuration with relevant variables. The data with beam energy 3 GeV are taken for the purpose of radiative corrections only and no attempt was made to keep $Q^2$ constant.

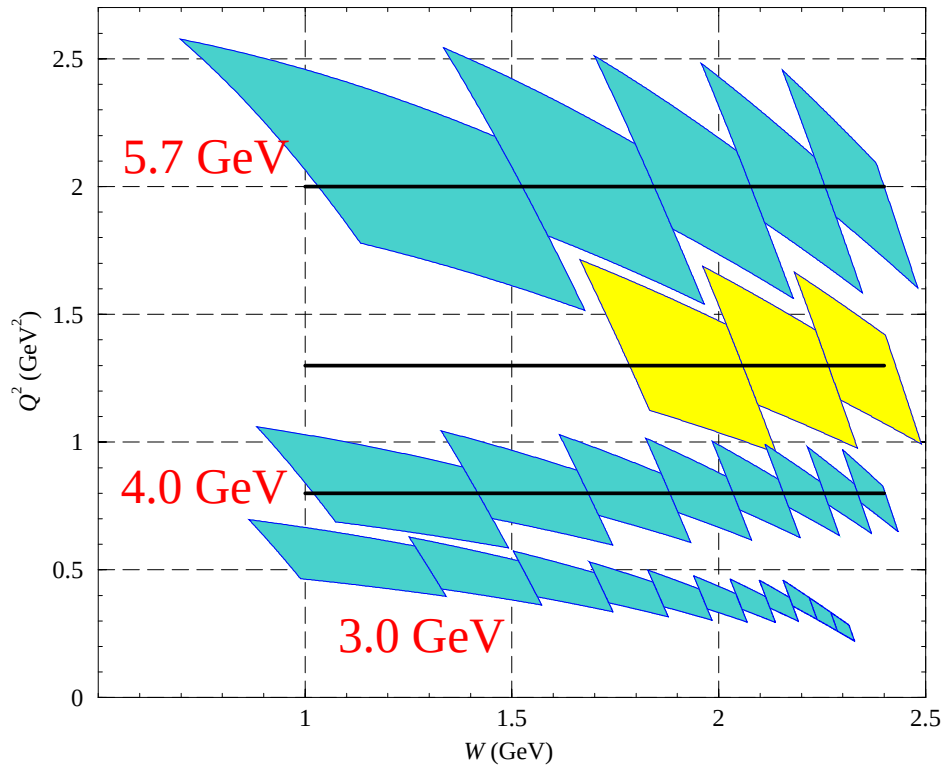


Figure 3: Actual coverage in $Q^2$ and $W$ for the transverse configuration. Light shaded region shows *extension* to JLab E01006. The three solid lines drawn correspond to constant $Q^2$ values at 2.0, 1.3 and 0.8 GeV$^2$.

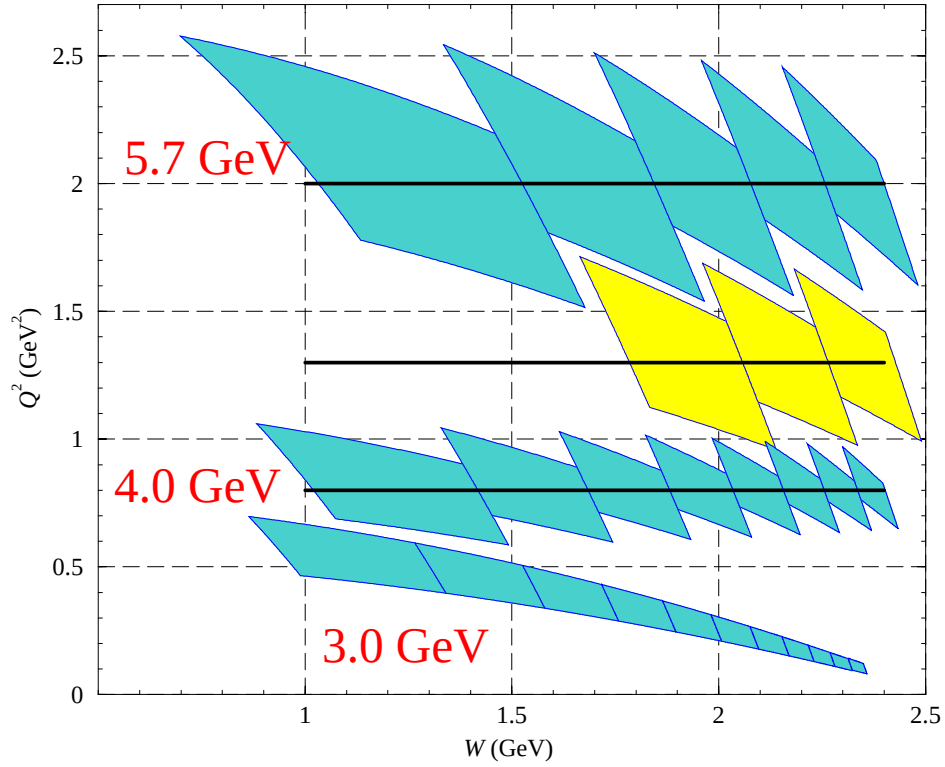


Figure 4: Actual coverage in $Q^2$ and $W$ for the longitudinal configuration. Light shaded region shows *extension* to JLab E01006. The three solid lines drawn correspond to constant $Q^2$ values at 2.0, 1.3 and 0.8 GeV$^2$.

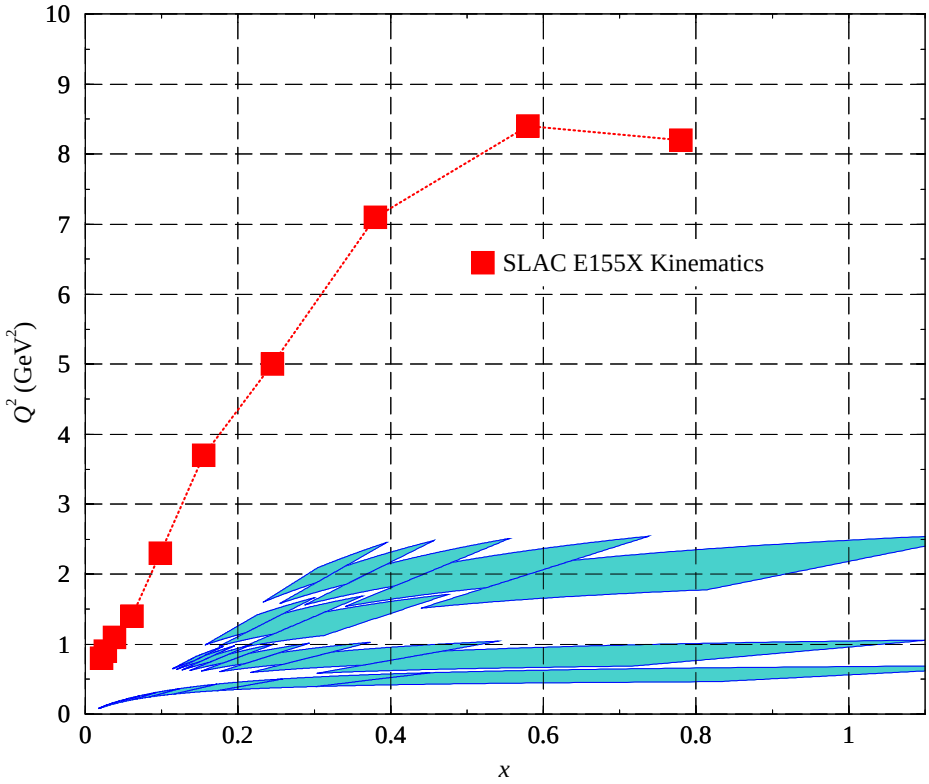


Figure 5: Comparison of kinematic coverage of SLAC E155X and the current proposal. SLAC E155X kinematics covers down to smaller $x$ than this proposal, but their $Q^2$ varies from 0.8 to 8.2 GeV$^2$. Their low $Q^2$ data can be used to complement our lack of data at small $x$ region.

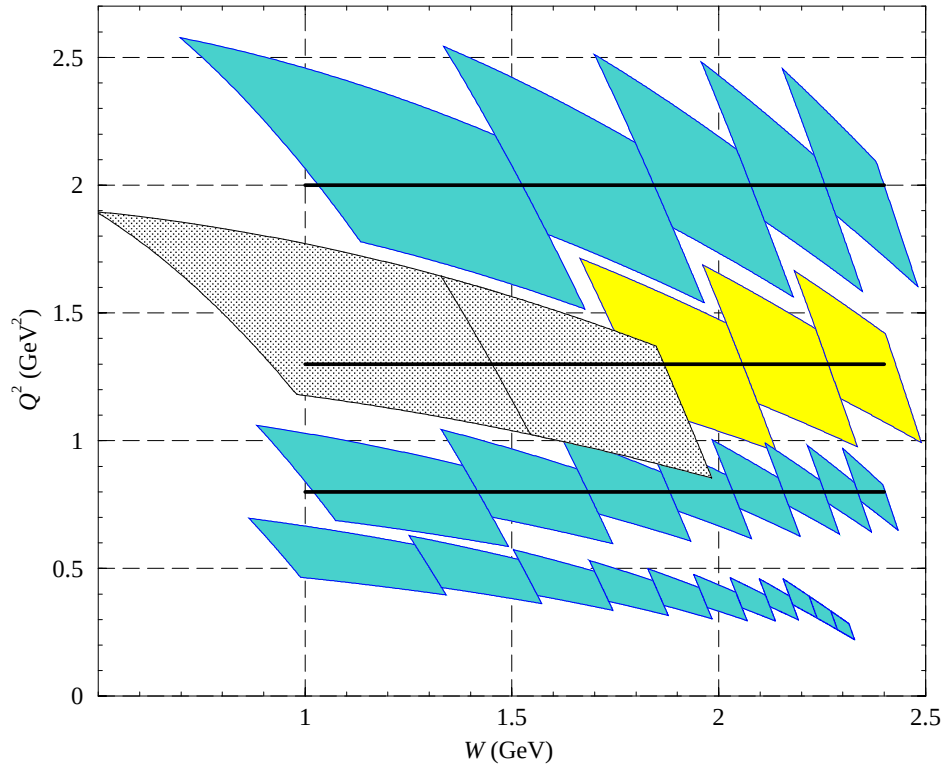


Figure 6: Comparison of kinematic coverage of JLab E01006 and the current proposal. Two dot filled region represents the coverage of JLab E01006 and light shaded regions are *extension* to that experiment included in this proposal.

# 4 Experimental Equipment

The equipment necessary for this proposal is similar to the previous experiment [22] and summarized below:

- Polarized electron beam with minimum 80% polarization and current between 60 to 100 nA. We need 3 beam energies: 5.70, 4.00 and 3.00 GeV.
- The Hall C Moller polarimeter to measure beam polarization.
- Beam raster system and the beam chicane.
- He bag for a dump line.
- The UVa-Basel-JLab polarized ammonia target with 70% $NH_3$ polarization with the beam.
- The Hall C HMS spectrometer in the HMS-1 point-to-point tune, $\geq$ 6.4 msr solid angle, $\sim$ 0.3% momentum resolution and $\pm$10% momentum acceptance.
- The normal HMS detector package to identify electrons and reject pions. The pion background was estimated using the EPC program [26] and $\pi^-/e-$ ratio was found to be less than 20 even in worst situations (high $W$ region). After the proper particle ID, the pion contamination will be negligible.
- Secondary Emissions Monitor (SEM) to measure the beam position at the target.

# 5 Counting Rates and Required Time

The counting rates of scattered electrons from the polarized target is given by

$$\mathrm{Rate} = \frac{\mathcal{L}\Delta E'\Delta\Omega}{f}\left(\frac{d^2\sigma}{dE'd\Omega}\right), \tag{24}$$

with the luminosity $\mathcal{L}$, spectrometer acceptance (both in momentum and solid angle) $\Delta E'\Delta\Omega$, dilution factor $f$ and proton cross section $\frac{d^2\sigma}{dE'd\Omega}$.

The actual counting rates have been estimated using QFS program by Lightbody and O'Connell. For proton luminosity, $1\times10^{35}\mathrm{cm}^{-2}\mathrm{Hz}$ has been used based

on the thickness of the target, $\sim 3 \times 10^{23}\mathrm{cm}^{-2}$ with 100nA beam current. For detectors, Hall C HMS standard parameters, $\pm 8$% momentum acceptance and 6.4 msr of angular acceptance have been used. Finally, the dilution factor for the frozen ammonia target ($^{15}NH_3$), an approximate value,

$$f = \frac{3}{3 + 15 + \epsilon} \simeq 0.13 \tag{25}$$

has been used for all the kinematics.

In addition to the rates on the proton, the total rates from all the materials in the target (H,Be,He,$N_2$) including their radiative tails have also been estimated. The total rates are always less than 1000Hz and even if we consider some pion rates, the counting rates are not limited by the DAQ.

Time required for each kinematics and configurations was adjusted to minimize the statistical error on $d_2(Q^2)$. Tables 3 and 4 give a summary.

| $E_{\rm beam}$ (GeV) | $E'$ (GeV) | Angle (°) | Proton Rate (Hz) | Time (Hr) | Comments |
|---|---|---|---|---|---|
| 5.70 | 4.2000 | 15.8492 | 0.12 | 87.51 | |
| | 3.5778 | 17.1551 | 0.17 | 33.80 | |
| | 3.0477 | 18.5568 | 0.13 | 12.93 | |
| | 2.5962 | 20.0596 | 0.08 | 8.44 | |
| | 2.2116 | 21.6655 | 0.05 | 6.88 | |
| 5.70 | 3.5000 | 13.5704 | 0.57 | 1.50 | |
| | 2.9815 | 14.6539 | 0.35 | 2.50 | |
| | 2.5398 | 15.8039 | 0.21 | 4.00 | |
| 4.00 | 3.2300 | 12.5998 | 1.19 | 134.12 | |
| | 2.7515 | 13.6122 | 0.92 | 17.65 | |
| | 2.3439 | 14.6773 | 0.60 | 5.44 | |
| | 1.9966 | 15.7912 | 0.36 | 1.77 | |
| | 1.7008 | 16.9468 | 0.22 | 1.09 | |
| | 1.4488 | 18.1331 | 0.14 | 0.89 | |
| | 1.2342 | 19.3349 | 0.09 | 0.83 | |
| | 1.0514 | 20.5267 | 0.06 | 0.83 | |
| 3.00 | 2.5000 | 12.5000 | 1.85 | 0.44 | Elastic |
| | 2.1296 | | 1.55 | 0.25 | |
| | 1.8141 | | 1.16 | 0.25 | |
| | 1.5454 | | 0.75 | 0.30 | |
| | 1.3164 | | 0.48 | 0.40 | |
| | 1.1214 | | 0.31 | 0.51 | |
| | 0.9553 | | 0.20 | 0.67 | |
| | 0.8137 | | 0.13 | 0.87 | |
| | 0.6932 | | 0.09 | 1.14 | |
| | 0.5905 | | 0.07 | 1.15 | |
| | 0.5030 | | 0.07 | 1.16 | |
| Total Time | | | | 327.32 | |

Table 3: Estimation of rates for the transverse configuration

| $E_{\rm beam}$ (GeV) | $E'$ (GeV) | Angle (°) | Proton Rate (Hz) | Time (Hr) | Comments |
|---|---|---|---|---|---|
| 5.70 | 4.2000 | 16.6188 | 0.12 | 21.62 | |
| | 3.5778 | 18.0169 | 0.17 | 4.12 | |
| | 3.0477 | 19.5352 | 0.13 | 0.77 | |
| | 2.5962 | 21.1842 | 0.08 | 0.26 | |
| | 2.2116 | 22.9755 | 0.05 | 0.25 | |
| 5.70 | 3.5000 | 14.6661 | 0.57 | 1.50 | |
| | 2.9815 | 15.8976 | 0.35 | 2.50 | |
| | 2.5398 | 17.2346 | 0.21 | 4.00 | |
| 4.00 | 3.2300 | 14.2945 | 1.19 | 53.64 | |
| | 2.7515 | 15.4949 | 0.92 | 2.48 | |
| | 2.3439 | 16.7966 | 0.60 | 0.38 | |
| | 1.9966 | 18.2100 | 0.36 | 0.25 | |
| | 1.7008 | 19.7448 | 0.22 | 0.25 | |
| | 1.4488 | 21.4121 | 0.14 | 0.25 | |
| | 1.2342 | 23.2236 | 0.09 | 0.25 | |
| | 1.0514 | 25.1920 | 0.06 | 0.25 | |
| 3.00 | 2.5000 | 15.32 | 1.85 | 0.44 | Elastic |
| | 2.1296 | | 1.55 | 0.25 | |
| | 1.8141 | | 1.16 | 0.25 | |
| | 1.5454 | | 0.75 | 0.25 | |
| | 1.3164 | | 0.48 | 0.25 | |
| | 1.1214 | | 0.31 | 0.27 | |
| | 0.9553 | | 0.20 | 0.29 | |
| | 0.8137 | | 0.13 | 0.31 | |
| | 0.6932 | | 0.09 | 0.32 | |
| | 0.5905 | | 0.07 | 0.32 | |
| | 0.5030 | | 0.07 | 0.33 | |
| Total Time | | | | 88.05 | |

Table 4: Estimation of rates for the longitudinal configuration

# 6 Estimation of Expected Accuracy

The statistical error on the BC sum rule have been estimated from Eq. 18. Explicitly, $g_2(x, Q^2)$ can be expressed in terms of $A_\parallel$, $A_\perp$ (or $A'_\perp$) and $\sigma_0$ as

$$g_2(x,Q^2) = \frac{Q^2}{4\alpha^2}\frac{M\nu^2}{E'(E+E')}\left(-A_\parallel + \frac{E+E'\cos\theta}{E'\sin\theta}A_\perp\right)\sigma_0 \quad (26)$$

$$= \frac{Q^2}{4\alpha^2}\frac{M\nu^2}{E'(E+E')}\times \quad (27)$$

$$\left[-\left(1+\frac{E+E'\cos\theta}{E'\sin\theta\tan\alpha}\right)A_\parallel + \left(\frac{E+E'\cos\theta}{E'\sin\theta\sin\alpha}\right)A'_\perp\right]\sigma_0, \quad (28)$$

where $\alpha = 80^\circ$.

Using this expression, it is straightforward to propagate statistical errors on $A_\parallel$ and $A'_\perp$ to $g_2(x, Q^2)$ and its integral.

The goal on statistics are set to achieve 2% statistical error on the asymmetries for each $\Delta E' = 50$ MeV bin for both configurations. This goal will give about 10% statistical error on the BC sum, about twice of corresponding systematic error.

With this statistical error, the expected statistical error on $\Gamma_2(Q^2)$ would be about $4 \times 10^{-3}$ and $2 \times 10^{-3}$ at $Q^2 = 0.8$ and 2.0 GeV$^2$, respectively. Compared to SLAC E155X measurements, these are 2 to 4 times better precision. Figures 7 and 8 show the expected statistical error on the BC sum rule and $xg_2(x, Q^2)$ from this proposal.

Expected systematic errors have been estimated based on the previous experiment [22] which uses similar techniques and analysis methods. In this proposal, the lowest energy data at 3 GeV are taken at different angles from the higher energy data. Although 3 GeV data will be used to anchor models, the systematic error from the radiation corrections will be bigger than the ideal situation where all the data are taken at the same angle. Using a conservative estimate based on the analysis of JLab E94010, 20% has been assumed for this contribution. At the same time, for the contribution from the unpolarized cross section, another conservative value of 5% has been used. Table 5 summarizes sources of systematic error.

Similar analysis has been done for $d_2(Q^2)$ and the result is shown in Figure 9.

| | |
|---|---|
| Beam polarization | 2% |
| Target polarization | 2.5% |
| Dilution factor | 2% |
| Nitrogen correction | $< 1\%$ |
| Pion contamination | $< 1\%$ |
| Dead time | $< 1\%$ |
| Radiative corrections | 20% |
| Errors from unpolarized cross section | 5% |
| **Total** | **21%** |

Table 5: Systematic error estimate

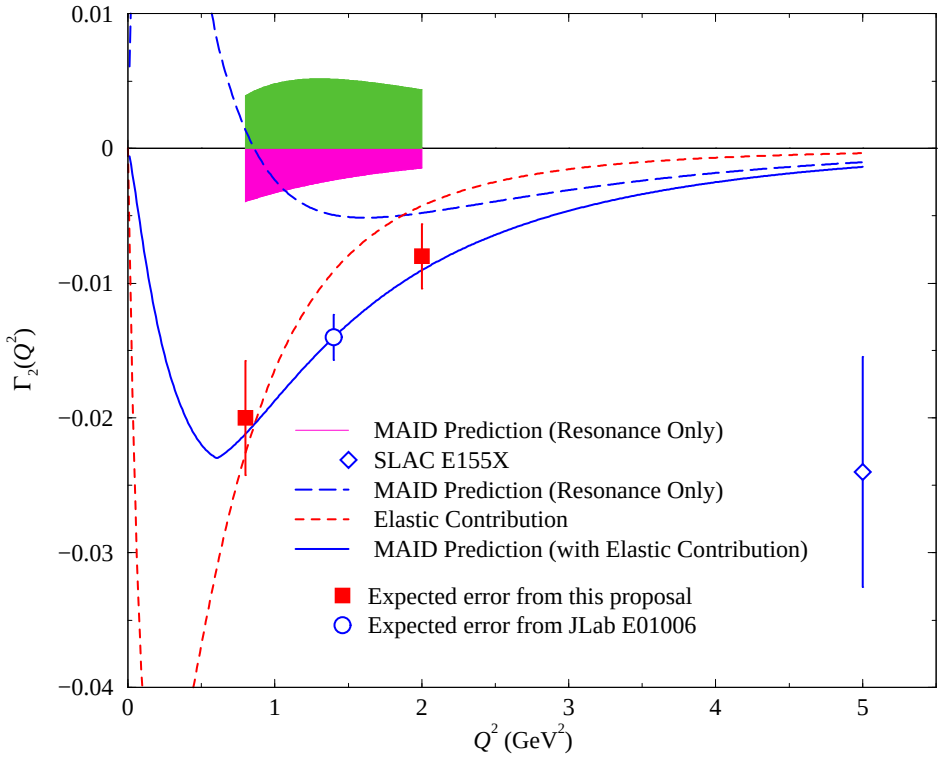


Figure 7: Expected statistical and systematic error for the BC sum rule from this proposal. The two square data points on the MAID curve show the expected statistical error at two values of $Q^2$. The open circle shows the expected error from JLab E01006. The dark gray band below the zero axis shows estimated experimental systematic error while the light gray band above the zero axis shows an estimate of DIS contribution from non-measured region using $g_2^{WW}(x, Q^2)$.

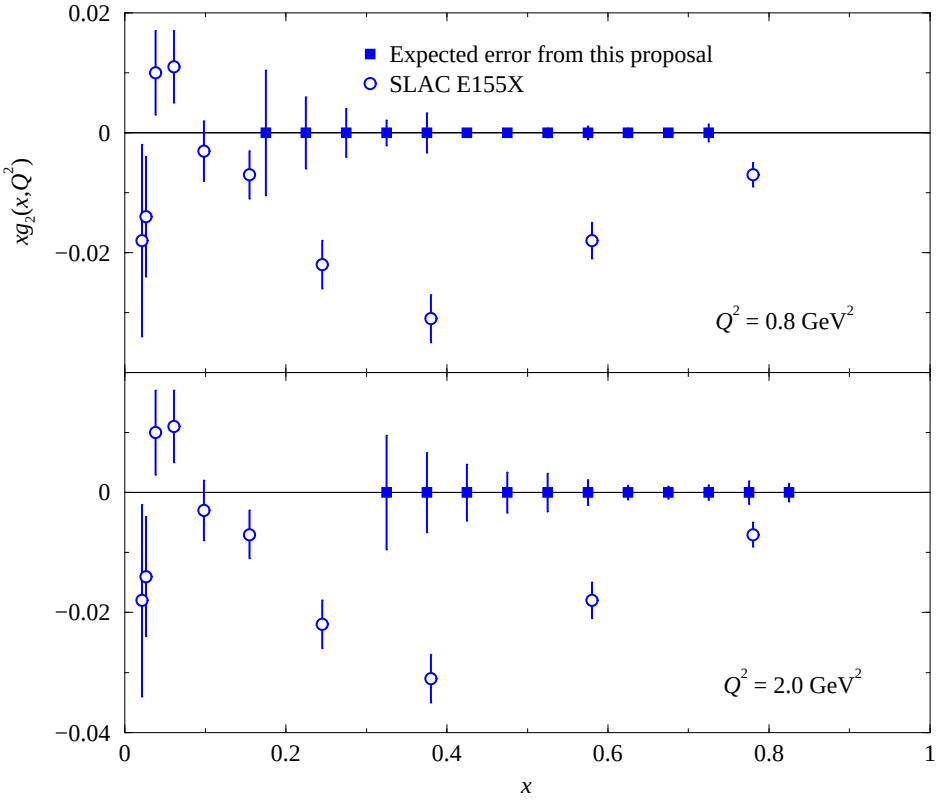


Figure 8: Expected statistical error for $xg_2(x, Q^2)$ compared with SLAC E155X for $Q^2$ = 0.8 and 2.0 GeV$^2$. In both frames, open circles show SLAC E155X data with error at $Q^2$ = 5.0 GeV$^2$ for comparison. Solid squares on the zero axis represent expected accuracy from this proposal.

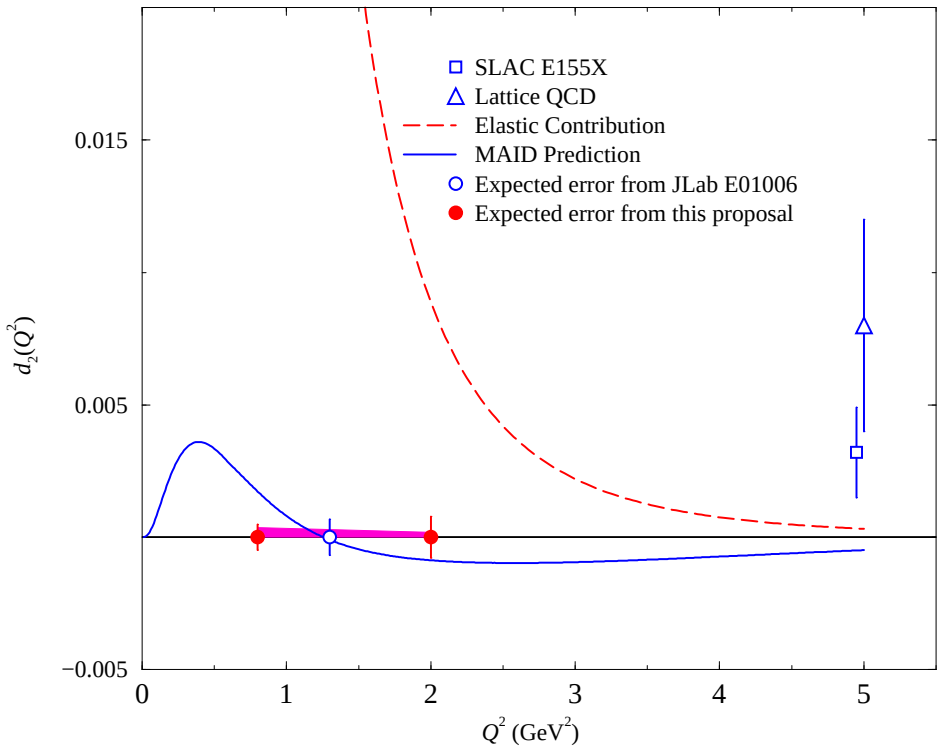


Figure 9: Expected statistical error for $d_2(Q^2)$ from this proposal. The two filled circles show the expected statistical error at two values of $Q^2$ while the open circle is the expected statistical error from JLab E01006. For $d_2(Q^2)$, due to the additional $x^2$ factor in the integral, the contribution from the non-measured region (generally small $x$) is negligible. The dark gray band close to zero axis shows estimated systematic errors.

# 7 Beam Time Request

The required time for data taking is summarized in Table 6 with the overhead estimate.

| Beam Energy (GeV) | Configuration | Time (Hrs) |
|---|---|---|
| 5.70 | Transverse | 157.56 |
| | Longitudinal | 35.02 |
| 4.00 | Transverse | 162.62 |
| | Longitudinal | 57.75 |
| 3.00 | Transverse | 7.14 |
| | Longitudinal | 3.28 |
| Total Data Taking | | 423.4 |
| Packing fraction measurement | | 20 |
| Moller measurement | | 20 |
| Target anneals | | 53 |
| Beam energy change | | 24 |
| Target material change | | 35 |
| Spectrometer Configuration Change | | 26 |
| Total overhead | | 165 |
| **Total Beam Time Request** | | **25 Days** |

Table 6: Run time and overhead estimate

# 8 Summary

We propose to make a precision measurement of $g_2(x, Q^2)$ for the proton at two values of $Q^2$, 0.8 and 2.0 GeV$^2$. The experiment will use three beam energies at 5.7, 4.0 and 3.0 GeV with various spectrometer angles from 12.5° to 25.2°. It will measure spin dependent asymmetries for the inclusive reaction $\vec{p}(\vec{e}, e')$ using polarized proton target in transverse and longitudinal configuration. Combined with the result on unpolarized proton cross sections, the spin structure functions functions $g_1(x, Q^2)$ and $g_2(x, Q^2)$ will be extracted. The Burkhardt-Cottingham sum rule for the proton will be tested and $d_2(Q^2)$ will be evaluated.

To do this measurement, we ask for 25 days of beam time with standard Hall C equipment.

# References


[1] E. Shuryak and A. Vainshtein, Nucl. Phys. **B201**, 141 (1982).

[2] R. L. Jaffe and Xiangdong Ji, Phys. Rev. D **43**, 724 (1991).

[3] S. Wandzura and F. Wilczek, Phys. Lett. **B72**, 195 (1977).

[4] B. W. Filippone and X. Ji, Adv. in Nucl. Phys. **26**, 1 (2001).

[5] X. Ji, in Proceeding of the Workshop on Deep Inelastic scattering and QCD, Editors: J. F. Laporte and Y. Sirois, Paris, France, 24-28 April, 1995 (ISBN 2-7302-0341-4).

[6] Chung Wen Kao, Thomas Spitzenberg and Marc Vanderhaeghen, hep-ph/0209241.

[7] J. D. Bjorken, Phys. Rev. **148**, 1467 (1966).

[8] J. D. Bjorken, Phys. Rev. D **1**, 1376 (1970).

[9] Hugh Burkhardt and W. N. Cottingham, Annals of Physics **56**, 453 (1970).

[10] M. Anselmino, A. Efremov and E. Leader, Phys. Rep. **261**, 1 (1995); Erratum-ibid, **281** 399 (1997).

[11] I. P. Ivanov *et al.,* Phys. Rep. **320** 175 (1999).

[12] R. L. Heimann, Nucl. Phys. **B64**, 429 (1973).

[13] G. Altarelli *et al.,* Phys. Lett. **B334** 187 (1994).

[14] Jiro Kodaira *et al.,* Phys. Lett. **B345** 527 (1995).

[15] Bodo Lampe and Ewald Reya, hep-ph/9810270.

[16] P. L. Anthony *et al.,* hep-ex/0204028

[17] V. Burkert, D. Crabb, R. Minehart, spokespersons, *Measurement of Polarized Structure Functions in Inelastic Electron Proton Scattering using CLAS*, JLab Experiment 91-023.

[18] S. E. Kuhn, spokesperson, *The Polarized Structure Function $g_1^n$ and the $Q^2$ dependence of the Gerasimov-Drell-Hearn Sum Rule for the Neutron*, JLab Experiment, 93-009.

[19] G. Cates, J.-P. Chen, Z.-E. Meziani, spokespersons, *Measurement of the Neutron ($^3$He) Spin Structure Function at Low $Q^2$: a Connection between the Bjorken and Drell-Hearn-Gerasimov Sum Rules*, JLab Experiment 94-010.

[20] Todd Averett, Wolfgang Korsch, spokespersons, *Search for Higher Twist Effects in the Neutron Spin Structure Function $g_2^n(x, Q^2)$*, JLab Experiment 97-103.

[21] J.-P. Chen, Z.-E. Meziani, P. Souder, spokespersons, *Precision Measurement of the Neutron Asymmetry $A_1^n$ at Large $x$ using CEBAF at 6 GeV*, JLab Experiment 99-117.

[22] O. Rondon, spokesperson, *Precision Measurement of the Nucleon Spin Structure functions in the Region of the Nucleon Resonances*, JLab Experiment 01-006.

[23] J.-P. Chen, S. Choi, N. Liyanage, *Measurement of Neutron ($^3$He) Spin Structure Functions in the Resonance Region*, JLab Experiment 01-012

[24] M. Amarian *et al.*, Phys. Rev. Lett. **89** 242301 (2002).

[25] C. Keppel, spokesperson, *Measurement of $R = \sigma_L/\sigma_T$ in the Nucleon Resonance Region*, JLab Experiment 94-110.

[26] J. W. Lightbody Jr. and J. S. O'Connell, Computers in Physics **2** 57 (1988).